Tensile Fracture of Coarse-Grained Cast Austenitic Manganese Steels

D. RITTEL and I. ROMAN

Tensile fracture of coarse-grained (0.25 to 1 mm) cast austenitic manganese (Hadfield) steels has been investigated. Numerous surface discontinuities nucleate in coarse slip bands, on the heavily deformed surface of tensile specimens. These discontinuities do not propagate radially and final fracture results from central specimen cracking at higher strains. On the microscopic scale, bulk voids nucleate during the entire plastic deformation and they do not coalesce by shear localization (*e.g.*, void-sheet) mechanism. Close voids coalesce by internal necking, whereas distant voids are bridged by means of small voids which nucleate at later stages of the plastic deformation. The high toughness of Hadfield steels is due to their high strain-hardening capacity which stabilizes the plastic deformation, and avoids shear localization and loss of load-bearing capacity. The observed dependence of measured mechanical properties on the specimen's geometry results from the development of a surface layer which characterizes the deformation of this coarse-grained material.

I. INTRODUCTION

HADFIELD (cast austenitic manganese) steels have long been known for their high toughness and hardening properties.[1-6] The tensile deformation of coarse-grained cast Hadfield steels has been characterized in a previous work, and the main macroscopic features observed were orange-peel formation, coarse slip bands, and lack of tensile necking.[7]

The present work is a characterization of tensile fracture mechanisms, in an attempt to understand both the high toughness of the material and the relationship between inhomogeneous deformation and subsequent fracture processes.

II. EXPERIMENTAL

The composition and microstructure of five heats of cast Hadfield steel employed in this study have been reported previously,[7,8] and will consequently be briefly described here. The steel was cast into keel blocks in order to optimize soundness. Carbides were dissolved by heating to 1050 °C, followed by quenching into water at room temperature. The resulting microstructure is austenitic. The typical grain size is widely distributed, and ranges from 0.25 to 1 millimeter. Some microporosity and residual interdendritic carbides (undissolved or reprecipitated during cooling from solution treatment) are discernible along with dendritic segregation (visible after repeated etching). Round (8 mm diameter) and flat square cross-section (6 mm side) tensile specimens were machined from the bottom of the keel. Final dimensions were obtained by fine grinding, in order to minimize the formation of a surface-hardened layer. Most of the tensile testing was performed on a closed loop servo-hydraulic machine, under load-control (10^4 N/min) at ambient temperature in air, employing an average of five specimens for each heat and geometry.

D. RITTEL, Doctoral Candidate, and I. ROMAN, Associate Professor and Head, are with Materials Science Division, Graduate School of Applied Science and Technology, The Hebrew University of Jerusalem, Jerusalem 91904, Israel.

Manuscript submitted September 18, 1987.

III. RESULTS

A striking difference is observed when the mechanical properties of round and square specimens are compared, as illustrated in Table I.* Both types of specimens possess nearly identical yield strength, whereas tensile elongation, reduction of area, and consequently true fracture strength are markedly higher for round specimens. Examination of the samples, during loading and after rupture, disclosed numerous cracks on the surface of both types of specimens (Figure 1). These cracks developed on planes almost perpendicular to the loading direction.

*The results shown in Table I are for heat MS4 in Reference 8, with 0.25 wt pct nickel added. These results illustrate the general trend which was observed in all investigated heats.

However, the average size of the cracks varied for each type of specimen. As can be seen from Figure 1, the cracks are visually detected on the surface of the square specimen (after 0.25 plastic strain), whereas they are hardly noticeable on the surface of the fractured round specimen. In both cases, the cracks are equally distributed along the gage of the specimen, and they develop parallel to coarse slip bands. Although the exact nucleation stage of the cracks was difficult to pinpoint, visual monitoring during tensile testing along with interrupted tests indicated that they were readily observable when the plastic strain exceeded 0.2. The microcracks were examined by scanning electron microscopy, prior to and after opening them up. Their shape is nearly

Table I. Typical Mechanical Properties of Coarse-Grained Cast Hadfield Steel (Heat MS4[8]) with 0.25 Wt Pct Nickel Added, as Determined from Round and Square Specimens

Specimen	Yield Strength (MPa)	True Fracture Strength* (MPa)	Reduction of Area (Pct)	Elongation (Pct)
Square	402 to 424	965 to 981	27 to 28	30 to 32
Round	404 to 408	1241 to 1471	32 to 40	49 to 59

*As fracture occurs without necking, true fracture strength is shown instead of ultimate tensile strength.

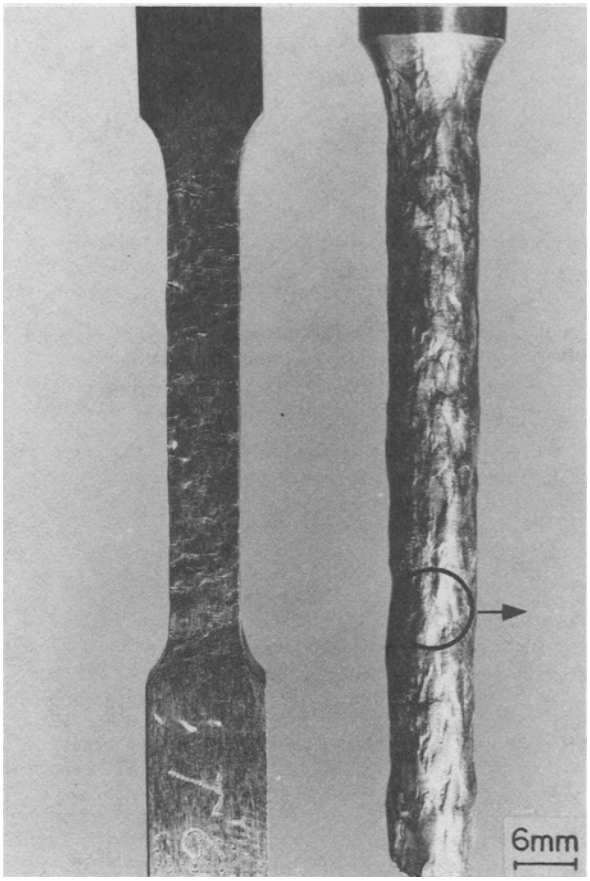

Fig. 1 — Square and round cross-sectioned tensile specimens. The square specimen underwent 0.25 plastic strain and the round specimen was strained to fracture.

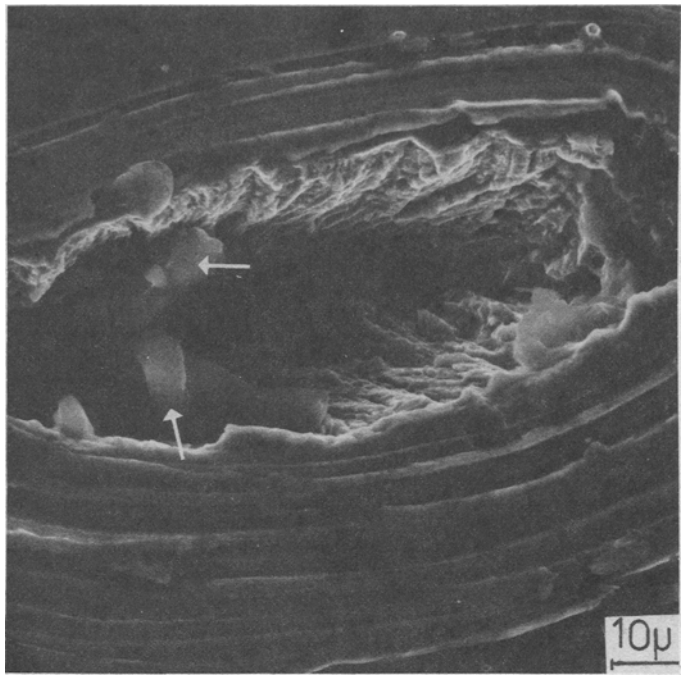

Fig. 2 — SEM micrograph showing a surface microcrack in a round tensile specimen, in the area marked in Fig. 1. The crack is elliptical, and particles (marked by arrows) are noticeable in the origin of the crack.

elliptical, as observed on the surface of the specimen (Figure 2). The topography contains microsteps, and in some cases particles (presumably carbides), such as those shown in Figure 2, could be found in the origin of the crack.

The fracture surface of the specimens was noted to be macroscopically flat (perpendicular to tensile axis), without marked shear lip. As stated in the introduction, fracture occurred without necking of the specimen. The main fracture surface topography of broken tensile specimens was found to comprise equiaxed dimples and microvoids in the center of the specimen. In the periphery, a step-like morphology made of elongated channels was observed (Figures 3 and 4). This two-layer topography was particularly remarkable for square specimens.

Longitudinal sections of specimens strained to various levels were prepared in order to investigate the surface microcracking and the fracture process. A large number of transgranular microcracks (typically 20 to 100 μm long according to the specimen) were observed along the gage length (Figures 1 and 5). However, these cracks did not propagate radially. Crack tips were blunted and a shear step could be observed at the origin of the crack.

Metallographic examination of the sections revealed a large number of elongated microvoids which nucleated around shattered foreign particles and carbides in the bulk of the material (Figure 6). These voids were observed at various stages of plastic deformation. They were uniformly distributed in the bulk of the specimen without any tendency to cluster around surface crack tips. Little, if any, void coalescence by shear localization mechanism, similar to the void-sheet mechanism reported by Cox and Low,[9] could be detected. Instead, close microvoids coalesced by internal necking after considerable reduction of the separating ligament. Careful examination of this ligament showed the presence of small shear steps on the periphery of the voids (Figure 7). Scanning electron examination of (nickel plated) main fracture profiles failed to reveal coalescence of microvoids underlying the highly strained fracture plane. Examination at higher magnifications revealed the existence of a population of small equiaxed microvoids of a wide range of sizes (Figure 8). These voids were homogeneously distributed in the bulk of the specimen. Here, too, the exact nucleation stage of these voids is difficult to pinpoint, but their equiaxed shape suggests that they nucleate at the later stages of the deformation, without significant growth that would result in their ovalization. As a result of their distribution, these voids could sometimes be observed to lie on a straight line connecting two elongated voids. Therefore, we suggest that distant elongated voids are bridged by these small voids, in the way depicted schematically in Figure 9.

A longitudinal section of a specimen strained close to fracture (about 0.3 plastic strain) is shown in Figure 10. In this specimen, a central crack (C) has developed in the vicinity of a large surface crack (S), in a plane where orange-peel (OP) amplitude was particularly noticeable inward. No interaction between the central and the surface crack (lying on roughly parallel planes perpendicular to the tensile axis) was noted. The central crack was found to result from the coalescence of large voids, and in this case void sheets were observable to a limited extent. It should be emphasized that central cracking was not observed in all other specimens that were strained to smaller strains (around 0.2). This indicates

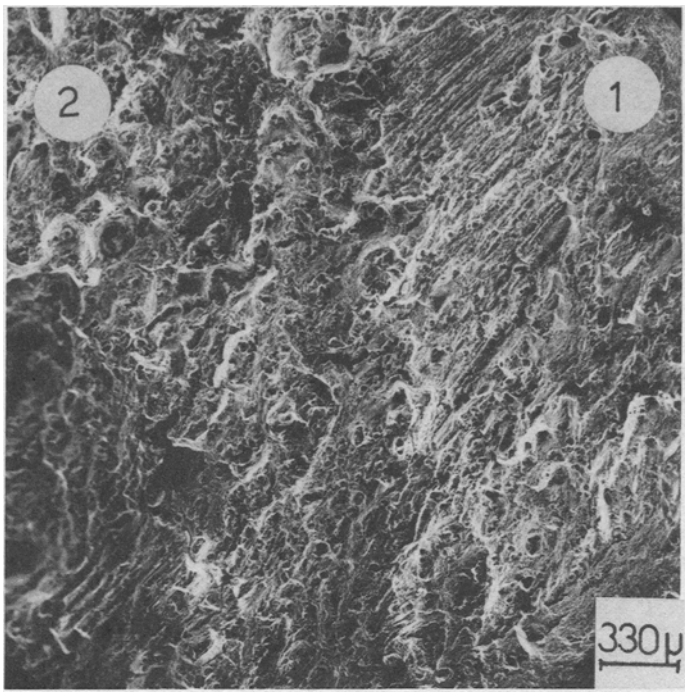

(*a*)

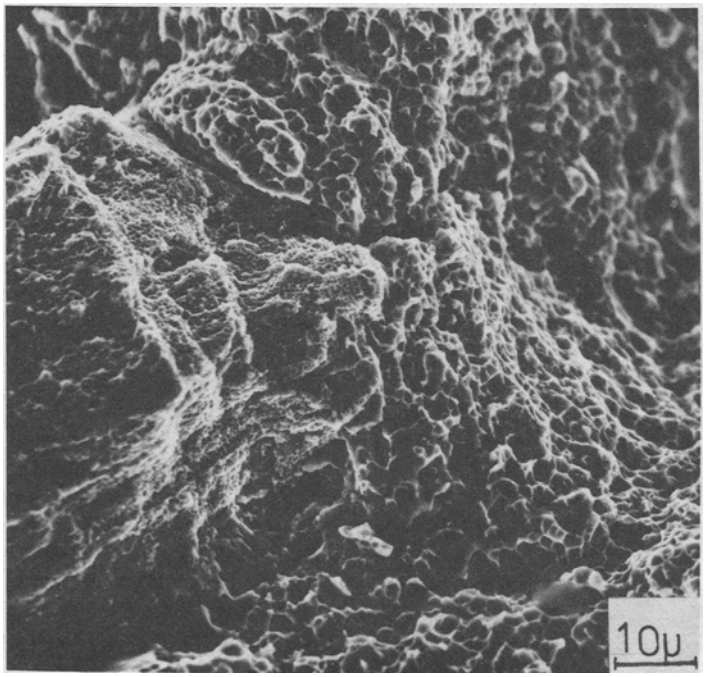

(*b*)

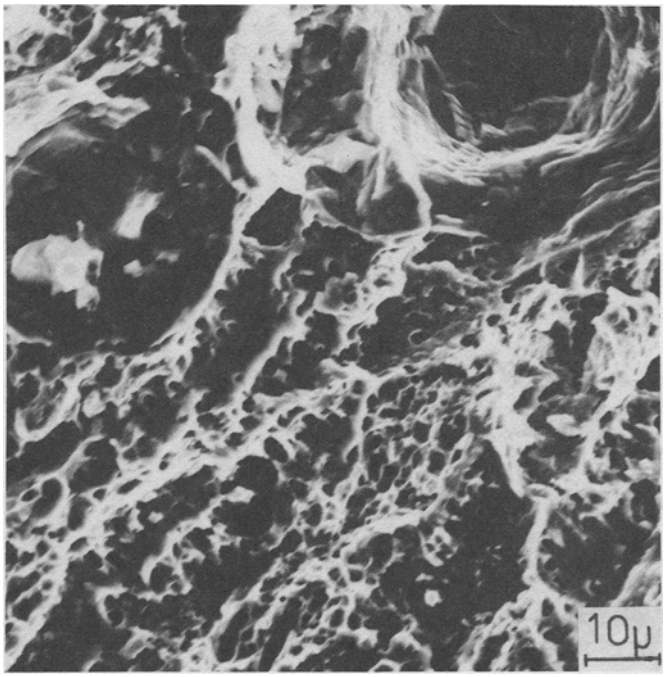

(*c*)

Fig. 3—SEM fractographs showing (*a*) typical topography of the fracture surface of a square tensile specimen: (1) external layer and (2) central layer; (*b*) magnification of region (1); (*c*) magnification of region (2).

that void coalescence responsible for macrocracking occurred at the later stages of deformation, close to final fracture.

IV. DISCUSSION

Experimental evidence indicates that tensile fracture of smooth Hadfield steel samples comprises early (low strain) surface cracking within coarse slip bands, and later central dimpled rupture. The mechanisms of void coalescence do not involve shear localization, as is commonly observed in the neck of ductile materials. For these materials, fracture progresses from the center of the specimen outward, yielding the well-known "cup and cone" morphology, whereas here the fracture surface is macroscopically flat. In addition,

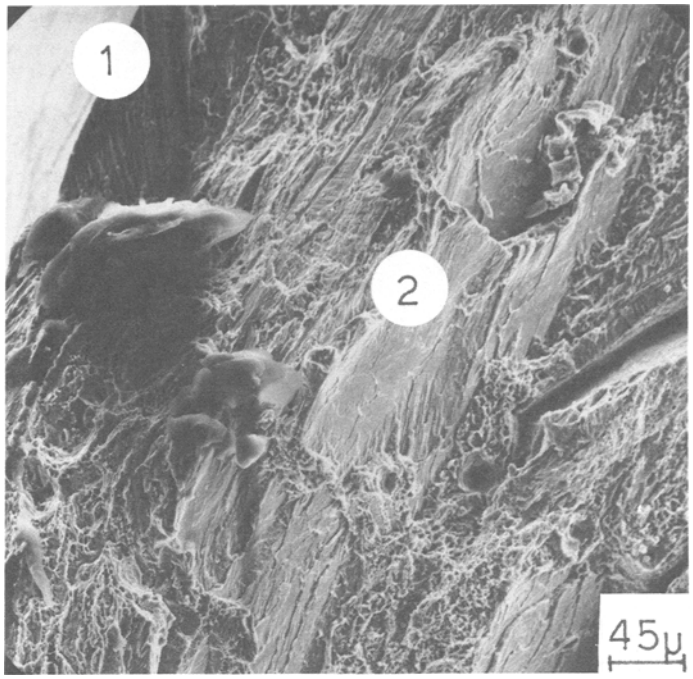

(*a*)

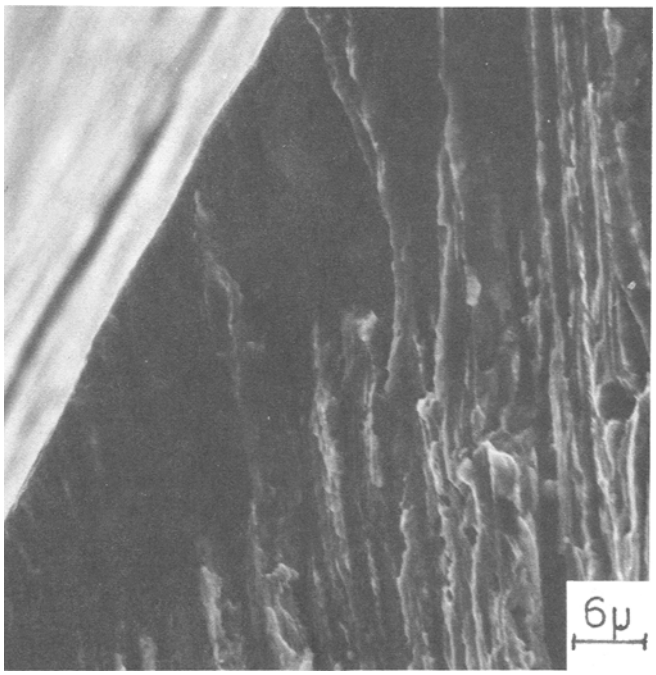

(*b*)

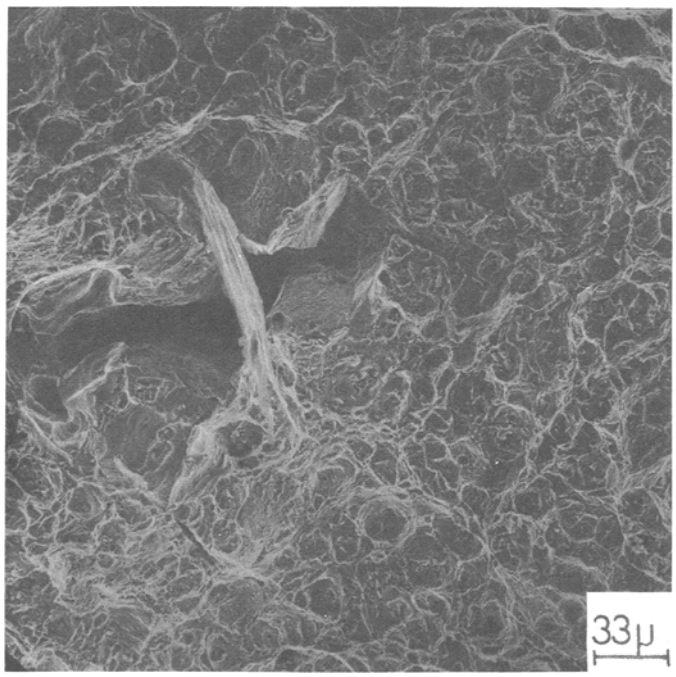

(*c*)

Fig. 4—SEM fractographs showing (*a*) typical topography of the fracture surface of a round tensile specimen: (1) external layer and (2) central layer; (*b*) magnification of region (1); (*c*) details of region (2).

we observed some peculiar phenomena which are related to the fracture process: development of a large number of circumferential nonpropagating microcracks and a dependence of the mechanical properties on the geometry of the tensile specimen. Accordingly, the following discussion is a detailed treatment of the fracture process and associated mechanisms.

A. *Fracture Process*

The initial fracture events in Hadfield steels involve localized surface cracking within coarse slip bands and nucleation of microvoids around carbides and particles. The nucleation of voids was observed at the early stages of

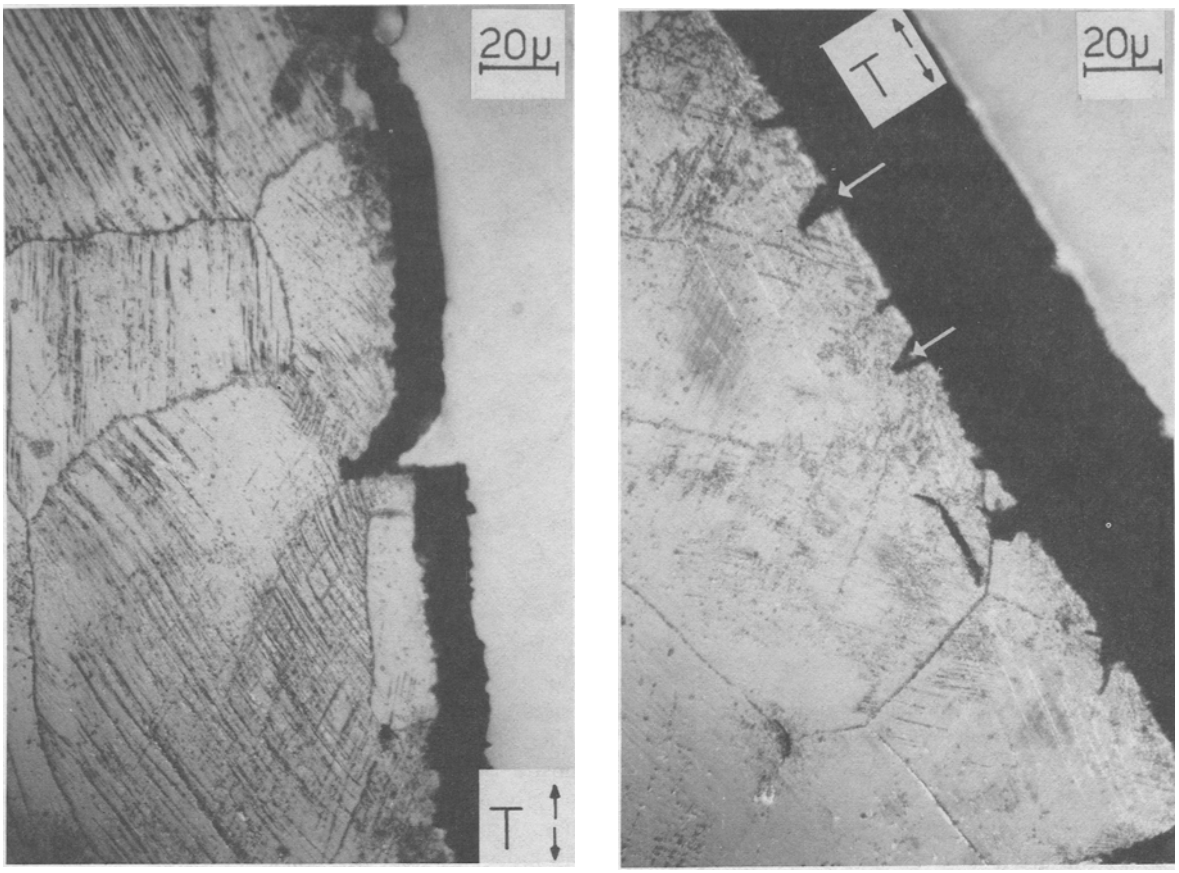

(*a*) (*b*)

Fig. 5 — Typical micrographs showing the microstructure of two (nickel-plated) longitudinal sections of fractured round tensile specimens. Note the nonpropagating transgranular surface microcracks (some of which are marked by arrows). *T* indicates tensile axis.

plastic deformation, as expected from a low yield strength material whose strain-hardening exponent at low strains is negligible.[1,7] Localized cracking is the natural consequence of the inhomogeneous plastic deformation of this class of steels, and similar features have been reported for aluminum alloys and steels.[10–14] It appears that these authors use a different terminology (coarse slip bands, superbands, and shear bands) to describe the same basic cracking phenomenon — that is, surface cracking within regions of localized plastic flow. This phenomenon, which is enhanced by the presence of foreign particles, has been associated with marked surface deformation.[11,13] Here, cracking remains confined to the surface of the specimen which is known to deform by orange-peel formation. In a previous report,[7] we suggested that orange-peel corresponds to a bifurcation of the plastic deformation into surface modes which decay exponentially from the free surface of the specimen.[15] Large displacements and strains are experienced by an outer region of the specimen, whose depth has been estimated to be αD (α-constant less than one, D-average grain size).[16] Such a region is characteristic of coarse-grained materials, and Fleischer *et al.* proposed that it possesses a lower yield strength than the bulk of the material.[16] Our fractographic observations show the existence of two distinct regions, one peripheral and one central. Both regions are characterized by ductile fracture features, and they indicate the operation

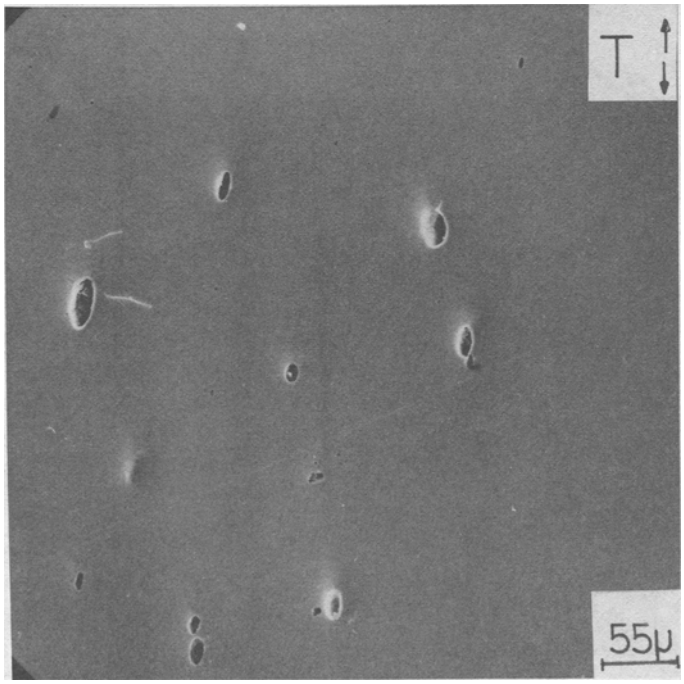

Fig. 6 — Typical micrograph of a longitudinal metallographic section of a fractured square tensile specimen Note the elongated microvoids. *T* indicates tensile axis.

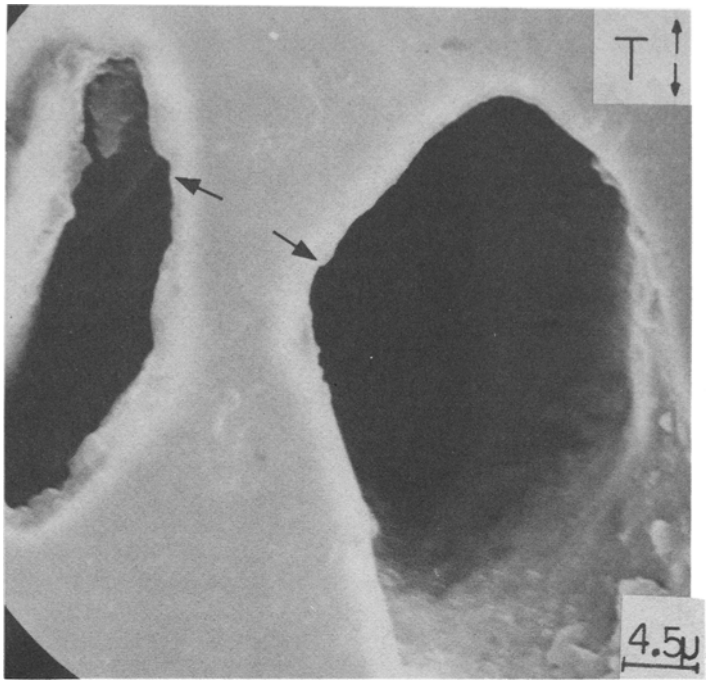

Fig. 7—Typical micrograph of a longitudinal metallographic section of a fractured square tensile specimen showing internal neck between elongated voids. The arrows point to shear steps on the periphery of the voids. *T* indicates tensile axis.

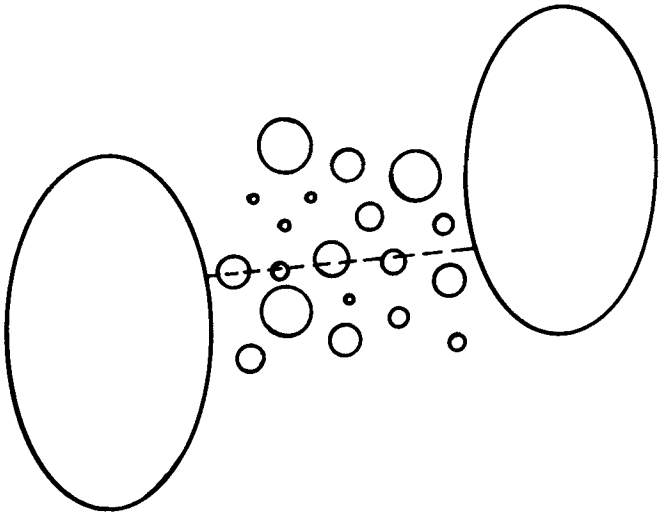

Fig. 9—Schematical representation of bridging mechanism between distant elongated voids by means of smaller equiaxed voids, such as those shown in Fig. 8. The dashed line indicates possible fracture path.

of two distinct types of rupture mechanisms, *i.e.*, surface shearing and central tensile overload. The nonpropagating nature of the surface cracks and the observation of central cracking indicate that these two processes are not related; that is, central cracking is not the direct continuation of surface cracking. This course of events is in contrast with former reports concerning surface cracking.[10,11] In these reports, surface cracks propagated radially and led to final fracture without necking. In addition, microvoids concentrated around crack tips, thus indicating a high level of local tensile triaxiality. We did not observe such features. Consequently, this comparison shows that one cannot define a distinct group of materials for which ductile fracture is simply induced by surface cracking.

The surface cracks are short with respect to a microstructural unit (*e.g.*, grain size), and they nucleate at strains corresponding to noticeable material hardening. Thus, the classical criterion for crack growth, where the fracture

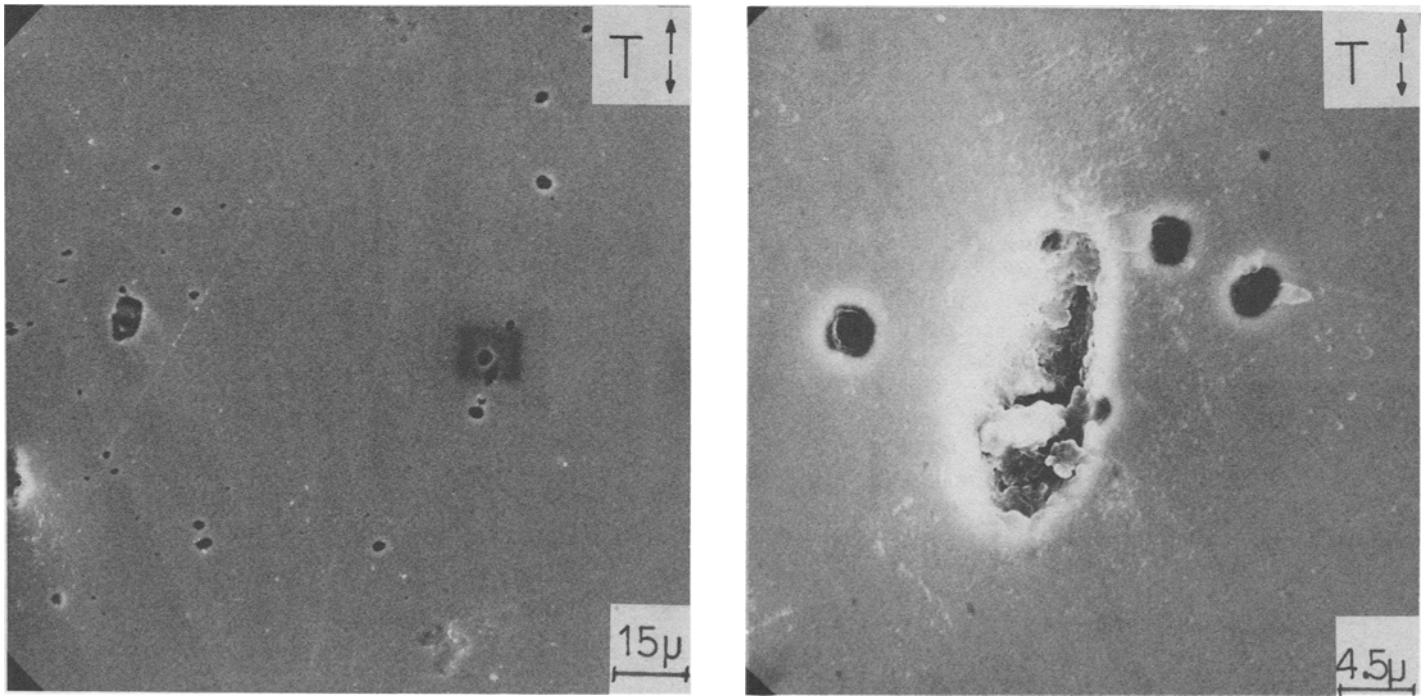

(*a*) (*b*)

Fig. 8—Typical micrograph of a longitudinal metallographic section of a fractured square tensile specimen showing (*a*) bulk distribution of small equiaxed voids; *T* indicates tensile axis; (*b*) small equiaxed voids which have developed in the vicinity of a larger elongated void. *T* indicates tensile axis.

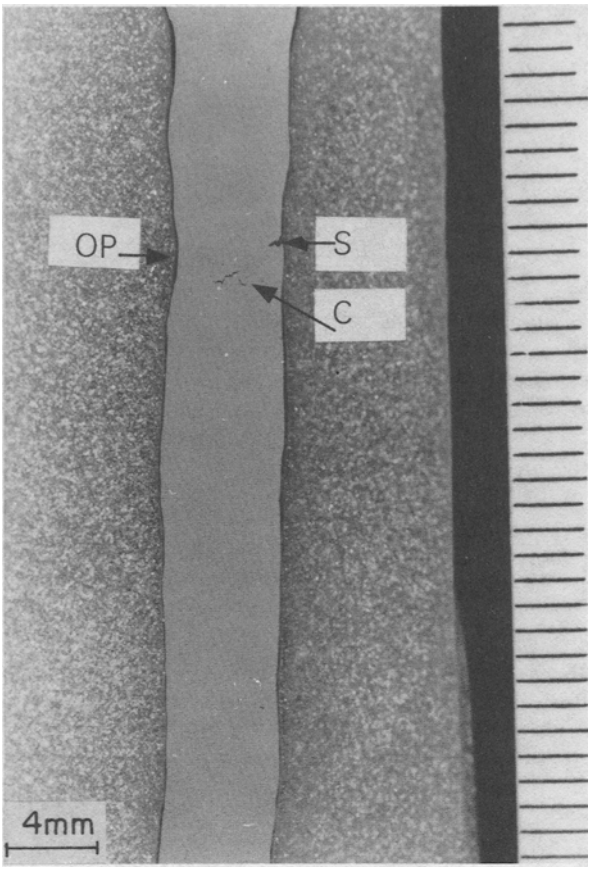

(*a*)

toughness (*e.g.*, *Jc*) is exceeded over some significant distance ahead of the crack tip, is obviously irrelevant here since the small flaw size would require the operation of extremely high stresses. In addition, the cracks nucleate in a surface region where the strain fields are highly nonuniform, as mentioned above. The high surface strains yield the observed elliptical crack shape. For the same reason, the crack propagation path is circumferential and remains confined to the surface of the specimen. In addition, the low concentration of microvoids near crack tips indicates a low degree of tensile triaxiality which is equivalent to the near absence of crack tip singular fields. Consequently, it is more appropriate to treat the nonpropagating surface cracks outside the context of fracture mechanics as voids or discontinuities in a highly viscous layer. These discontinuities grow by a shear mechanism whose extent is, of course, limited by grip constraint effects (enforcing specimen alignment) and by the local orange-peel amplitude. In conclusion, surface discontinuities do not dominate the fracture process in the sense of fracture mechanics effects, but they most probably weaken the surface layer in which they nucleate. Instead, ultimate fracture occurs by central cracking of the specimen without marked interaction with the preceding surface discontinuities. As a result there is no shear lip on the fracture surface.

B. *Fracture Mechanisms*

It is interesting to note that Hadfield steels fracture without necking. The load-bearing capacity increases steadily with deformation, even when the surface gets markedly rumpled, cracked, and the bulk of the specimen contains

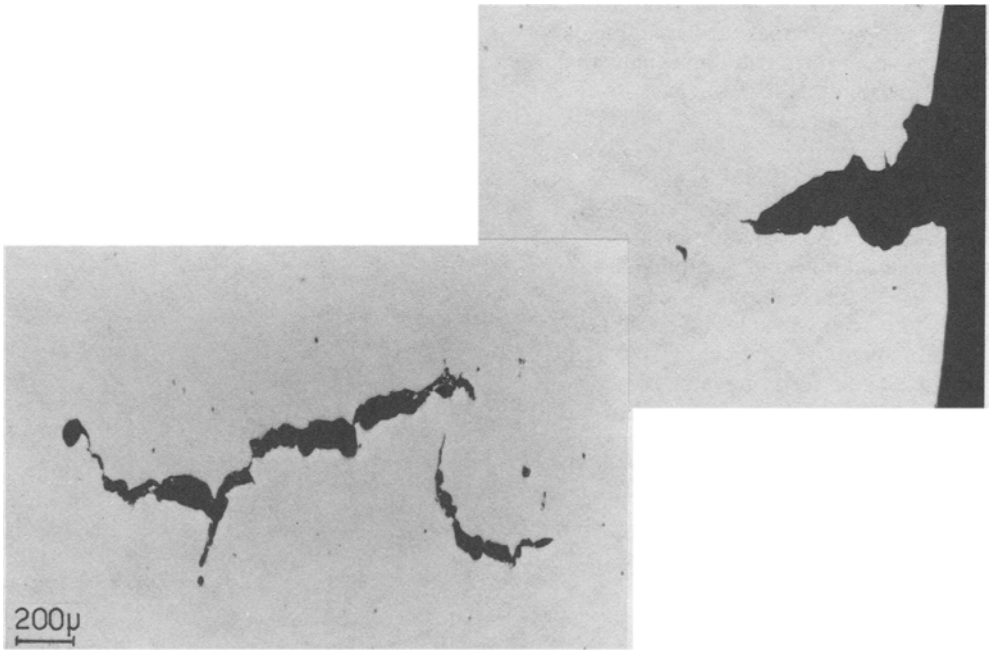

(*b*)

Fig. 10—(*a*) Typical micrograph of a diagonal longitudinal section of a square tensile specimen strained nearly to fracture. Central (C) and surface cracking (S) are noticeable in a region of marked orange-peel amplitude (OP). (*b*) Micrographs at higher magnification of the central and surface cracks. Lack of shear localization between crack tips is noticeable.

numerous microvoids. This remarkable behavior can be explained only in terms of the high strain-hardening capacity of the material. This capacity increases rapidly with strain,[1,7] and we propose that strain-hardening compensates the loss of load-bearing capacity associated with the above-mentioned factors.

Another aspect of the material toughness is related to the mechanism of void coalescence. While different models have been proposed to describe void growth and coalescence (see, *e.g.*, References 17 through 19), they all imply a decrease in load-bearing capacity associated mostly with tensile necking. This capacity tends gradually to zero as a critical void volume fraction is approached. Consequently, such models do not adequately describe the fracture of Hadfield steels and the volume fraction cannot be used as a fracture criterion.[20] It rather seems that the critical point of the fracture process concerns the type of mechanism of void coalescence. The lack of shear localization between voids is understood by assuming that very fine particles of some finite size are required to provide nucleation sites for the fine dimples lying in a localization band (*e.g.*, void sheet[9]). Although it is not clear whether these particles are a prerequisite for localization (see, *e.g.*, Reference 21), it seems that fine carbides in the austenitic phase cannot provide such sites, resulting in delayed void coalescence. This is probably the reason why no interaction was observed between the tips of the interior and surface cracks. Such observation is surprising for a material whose deformation is so grossly inhomogeneous,[7] but here again it appears that the high strain-hardening capacity of the material has a stabilizing influence on flow localization and fracture. Similar observations have been reported for sintered titanium and titanium alloy.[22] Deformation and fracture of the material are therefore related to its hardening characteristics in the following way: low initial hardening promotes coarse slip band formation and probably surface cracking, along with opening of bulk voids, whereas steadily increasing hardening prevents their coalescence by shear localization mechanism. In the same spirit, we propose that this lack of shear localization is partly responsible for the arrest of surface discontinuities, the propagation of which would otherwise be enhanced by localization between crack-tip and bulk voids.

The dynamics of void growth and coalescence process are slowed down by two factors: firstly, the absence of stress triaxiality associated with necking, and secondly the high strain-hardening capacity of the material.[17] The macroscopic locus of the fracture path can thus be explained as follows: for planes with marked orange-peeling, the hydrostatic pressure is locally elevated, resulting in increased void growth rate and probability for coalescence. Consequently, central cracking is observed in the area of the specimen where the orange peel amplitude is markedly higher, thus creating a sort of diffuse neck. For the same reason, when mixed kinds of orange peel (coarse and fine) occurred in the same specimen (resulting from nonuniform grain-size[7]), fracture took place in the coarser area.

C. *Geometrical Effects*

The influence of the specimen geometry on the mechanical properties has been related to the existence of a weak surface layer in the specimens. We now calculate the relative volume occupied by such layer of thickness αD, for a round (radius R) and a square (side a) specimen (Figure 11). For the round specimen,

$$\frac{V\text{out}}{V\text{in}} = \frac{(2\alpha RD - \alpha^2 D^2)}{(R - \alpha D)^2}, \qquad [1]$$

And for the square specimen,

$$\frac{V\text{out}}{V\text{in}} = \frac{4\alpha D(a - \alpha D)}{(a - 2\alpha D)^2}. \qquad [2]$$

Here, Vout and Vin stand for the volume of the surface layer and the remaining volume of the specimen, respectively. Experimental values can be substituted for D (1 mm), R (4 mm), and a (6 mm) in Eqs. [1] and [2]. As to α, there is no reason to suppose *a priori* that it is specimen dependent, and therefore the value of 0.7[16] can be used here yielding the following results:

$$\frac{V\text{out}}{V\text{in}} = \begin{cases} 0.47 \text{ for the round specimen} \\ 0.70 \text{ for the square specimen} \end{cases}$$

Keeping in mind that the external layer possesses a lower strength than the interior one due its deformation mode[16] and extensive cracking, it is understood that the square specimen with a proportionally greater surface layer will require less work to fracture, resulting in premature failure when compared with the round specimen of identical grain size. In other words, the surface layer of the specimen limits its ductility and consequently its fracture strength. The numerical results shown above represent an "upper bound" limit, due to the large grain size employed. In addition, it is easily verified that the difference between both types of specimens decreases with decreasing grain size, and is no longer perceptible for grain sizes of less than 0.25 mm. Therefore the specimen dependent mechanical properties stem from a purely geometrical effect related to the development of a surface layer. The extent to which such surface layer affects mechanical and fracture properties is determined by the cross section of the specimen (for a given grain size). Consequently, the round specimen is moderately affected by this layer, whereas the square specimen tends to behave as a "surface" specimen.

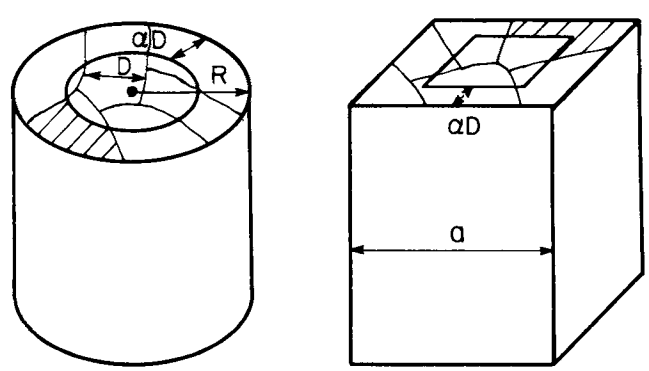

Fig. 11—Schematical representation of surface layers (thickness αD) in round (radius R) and square (side a) tensile specimens with average grain size D.

V. CONCLUSIONS

Tensile fracture of coarse-grained Hadfield steels is a two-step process; it involves localized formation of nonpropagating surface discontinuities for strains of about 0.2, and central cracking of the specimen near the fracture strain. There is no direct interaction between these two types of cracking. Surface cracking occurs along with orange-peel formation which characterizes the inhomogeneous plastic deformation of this material. This phenomenon weakens a surface layer of the specimen, whose depth is proportional to the average grain size. The existence of such layer limits the overall ductility and fracture strength of the specimen. Accordingly, for a given coarse grain size (exceeding 0.25 mm), mechanical properties are dependent on the geometry of the specimen.

The high toughness of the material is associated with its resistance to void coalescence by a shear localization mechanism. This results from the high strain-hardening capacity of Hadfield steels which is also responsible for the steadily increasing load-bearing capacity until fracture. The overall process of void nucleation and growth is slowed down by lack of tensile necking and by the high material hardening. Orange-peel modulates the local hydrostatic pressure by creating diffuse necks, in one of which central cracking occurs. Central cracking is responsible for the ultimate fracture of the specimen.

ACKNOWLEDGMENT

The authors would like to express their gratitude to Urdan Associated Steel Foundries for the provision of the experimental material.

REFERENCES

1. H. C. Doepken: *J. of Metals*, Feb. 1952, pp. 166-70.
2. W. N. Roberts: *Trans. TMS-AIME*, 1964, vol. 230, pp. 372-77.
3. K. S. Raghavan, A. S. Sastri, and M. J. Marcinkowski: *Trans. TMS-AIME*, 1969, vol. 245, pp. 1569-75.
4. D. J. Drobjnak and J. Gordon Parr: *Metall. Trans.*, 1970, vol. 1, pp. 759-65.
5. Y. N. Dastur and W. C. Leslie: *Metall. Trans. A*, 1981, vol. 12A, pp. 749-58.
6. P. H. Adler, G. B. Olson, and W. S. Owen: *Metall. Trans. A*, 1986, vol. 17A, pp. 1725-37.
7. D. Rittel and I. Roman: Hebrew University of Jerusalem, unpublished research, 1988.
8. D. Rittel and I. Roman: *Fatigue Life—Analysis and Prediction*, V. S. Goel, ed., ASM, 1986, pp. 109-16.
9. T. B. Cox and J. R. Low, Jr.: *Metall. Trans.*, 1974, vol. 5, pp. 1457-70.
10. R. J. Price and A. Kelly: *Acta Metall.*, 1964, vol. 12, pp. 979-92.
11. G. T. Hahn and A. R. Rosenfield: *Metall. Trans. A*, 1975, vol. 6A, pp. 653-68.
12. K. Tanaka and J. W. Spretnak: *Metall. Trans.*, 1973, vol. 4, pp. 443-54.
13. O. A. Onyewuenyi and J. P. Hirth: *Scripta Metall.*, 1984, vol. 18, pp. 455-58.
14. O. A. Onyewuenyi and J. P. Hirth: *Metall. Trans. A*, 1982, vol. 13A, pp. 2209-18.
15. R. Hill and J. W. Hutchinson: *J. Mech. Phys. Solids*, 1975, vol. 23, pp. 239-65.
16. R. L. Fleischer and W. F. Hosford, Jr.: *Trans. TMS-AIME*, 1961, vol. 221, pp. 244-47.
17. A. Argon and F. McClintock: *Mechanical Behavior of Metals*, Addison-Wesley, 1966.
18. A. Needleman and V. Tvergaard: *Finite Elements—Special Problems in Solid Mechanics*, Prentice-Hall Inc., 1984, vol. V.
19. V. Tvergaard and A. Needleman: *Acta Metall.*, 1984, vol. 32, no. 1, pp. 157-69.
20. D. Rittel and I. Roman: *Int. J. Fracture*, 1987, no. 35, pp. R61-R64.
21. J. R. Rice: in *Theoretical and Applied Mechanics*, W. T. Koiter, ed., North-Holland Pub. Co., 1976, pp. 207-20.
22. R. J. Bourcier, D. A. Koss, R. E. Smelser, and O. Richmond: *Acta Metall.*, 1986, vol. 34, no. 12, pp. 2443-53.